Self-Propelled Dropwise Condensate on Superhydrophobic Surfaces

Jonathan B. Boreyko and Chuan-Hua Chen*

Department of Mechanical Engineering and Materials Science, Duke University, Durham, North Carolina 27708, USA

(Received 25 May 2009; published 26 October 2009)

In conventional dropwise condensation on a hydrophobic surface, the condensate drops must be removed by external forces for continuous operation. This Letter reports continuous dropwise condensation spontaneously occurring on a superhydrophobic surface without any external forces. The spontaneous drop removal results from the surface energy released upon drop coalescence, which leads to a surprising out-of-plane jumping motion of the coalesced drops at a speed as high as 1 m/s. The jumping follows an inertial-capillary scaling and gives rise to a micrometric average diameter at steady state.

DOI: 10.1103/PhysRevLett.103.184501 PACS numbers: 47.55.dr

Dropwise condensation occurs on a surface not wetted by the condensate [1] and is typically 10 times more effective than filmwise condensation in phase-change heat transfer [2,3]. To achieve effective dropwise condensation, condensate must be quickly removed from the surface as it accumulates; otherwise, large drops will inhibit heat transfer due to the poor thermal conductance of liquid condensate [3]. Gravitational removal is the most common mechanism, but this approach depends on the orientation and only affects drops with a diameter comparable to the capillary length [4]. Here, we show that condensate drops can be autonomously removed on a superhydrophobic surface without any external forces; we also show that the average drop radius at steady-state condensation is 3 decades smaller than the capillary length. The spontaneous motion is powered by the surface energy released upon drop coalescence and is unique in that out-of-plane jumping results from in-plane coalescence. A similar mechanism is used by ballistospore mushrooms to discharge a spore from the tip of its sterigma, a process triggered by the coalescence of the Buller's drop (condensate at the base of the spore) with the wetted spore [5–7]. We believe the jumping motion reported here is underlying recent reports of rapid drop movement upon coalescence on synthetic and natural superhydrophobic surfaces [8–10].

A superhydrophobic substrate, composed of two-tier roughness with carbon nanotubes deposited on silicon micropillars and coated with hexadecanethiol, was prepared in the same manner as structure B_{mn} in [8]. As a control case, a smooth silicon substrate coated with hexadecanethiol was also used. The substrates were placed on a horizontally oriented copper plate controlled at $5.5 \pm 0.5\,^{\circ}\mathrm{C}$ by a circulating chiller. A thin film of water was used to reduce the contact resistance between the substrates and the cold plate. The laboratory temperature was measured to be $19\,^{\circ}\mathrm{C}$ with a relative humidity of 74% (dew point $= 14\,^{\circ}\mathrm{C}$). Video imaging of water vapor condensing from the air was captured with a Phantom v7.1 camera attached to a Nikon LV150 or an Infinity K2 microscope for top-down or side-view imaging.

Horizontally oriented hydrophobic and superhydrophobic substrates were chilled and the resulting condensation process was captured (Fig. 1). Figure 1(a) shows conventional dropwise condensation on the smooth hydrophobic surface, while Fig. 1(b) shows condensation on the superhydrophobic surface. In lack of an external drop removal mechanism, the drops continued to grow on the hydrophobic surface. In contrast, the condensate drops on the superhydrophobic surface were autonomously removed, as evident from the large ''dry'' area at 20 min [Fig. 1(b)].

Quantitative analysis of the condensation process is shown in Fig. 2. The surface coverage (ϵ^2) is the ratio of the projected surface area covered by the drops over the substrate area. The surface coverage reaches a plateau of $\epsilon^2 \approx 0.4$ for the superhydrophobic surface, smaller than $\epsilon^2 \approx 0.6$ for the hydrophobic surface [Fig. 2(b)]. The consequence of the autonomous drop removal is even more pronounced for the average drop diameter, $\langle 2r \rangle$, which plateaus on the superhydrophobic surface but continues to grow on the hydrophobic surface [Fig. 2(a)].

The temporal evolution of the average drop diameter follows a power law [11],

$$\langle 2r \rangle \sim t^{\alpha}, \tag{1}$$

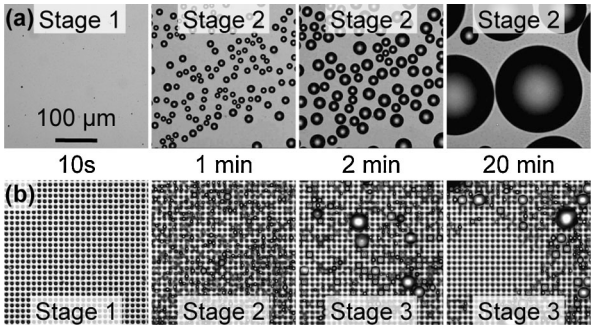

FIG. 1. (a) Dropwise condensation on a smooth hydrophobic substrate and (b) on a rough superhydrophobic substrate where the micropillars are visible. Both substrates were horizontally oriented. Stages 1–3 of the condensation process characterize the initial nucleation, immobile coalescence, and mobile coalescence, respectively. See supplemental videos S1, S2 in [33].

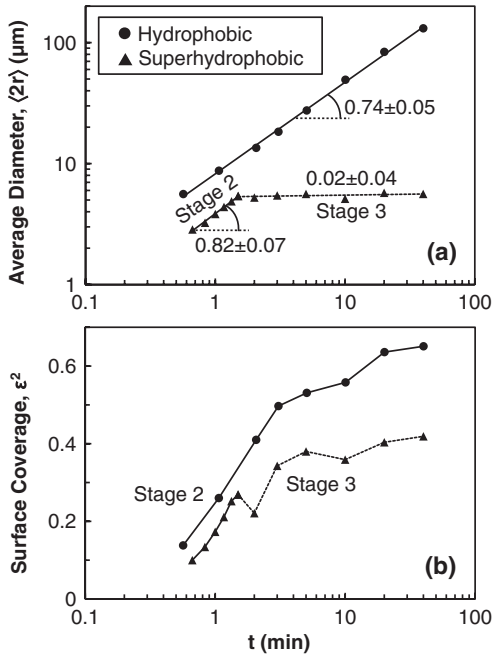

FIG. 2. Statistics of the temporal evolution of condensate patterns in Fig. 1: (a) the average drop diameter, where the slopes shown are the power law exponent α; (b) the surface coverage, which reached a plateau for both the hydrophobic and superhydrophobic surfaces but fluctuated because of the small field of view. Stage 3 is the mobile coalescence stage exclusive to superhydrophobic condensation, denoted by the dashed lines. Time 0 corresponds to the first visual appearance of condensate drops [12], and the error bars are the 95% confidence intervals of the exponential fit.

where t is the time and α is the growth law exponent depending on the stage of condensation. Without external forces, two stages of condensation were observed on the hydrophobic surface, while an additional third stage was observed for the superhydrophobic surface as a result of the autonomous removal [Fig. 2(a)]:

Stage 1: initial growth without coalescence.—At the first stage, drops nucleated and grew without significant interactions, and the initial surface coverage was negligible. Because of the initial transient cooling of the cold plate, we could not accurately determine the power law in the first 30 s [12]; however, the $1/3$ law is expected on both hydrophobic and superhydrophobic surfaces [13–15].

Stage 2: immobile coalescence.—At the second stage, the surface coverage was large enough for the condensate to frequently coalesce together, but the center of mass of the merging drops did not change appreciably before and after coalescence. On the hydrophobic surface, the growth followed a power law with $\alpha = 0.74 \pm 0.05$. This growth law is consistent with the approximate 0.75 law measured for breath figures [16,17]. The discrepancy with the theoretical approximation of $\alpha = 1$ [18] could be explained by the transient in surface temperature [12,17] as well as other simplifications discussed in [18]. On the superhydrophobic surface, coalescence did not begin until $t \approx 40$ s when $\langle 2r \rangle \approx 3$ μm. Droplet growth followed a power law with $\alpha = 0.82 \pm 0.07$, close to growth rates observed on textured surfaces [14,15]. While immobile coalescence with continuous power law growth was the steady-state behavior on the hydrophobic surface, the condensation on the superhydrophobic surface entered a third stage at 90 s.

Stage 3: mobile coalescence.—When the average drop diameter on the superhydrophobic surface reached a threshold value, coalescence led to the mobilization and rapid removal of the merged drops from the surface. This autonomous removal resulted in a power law exponent of $\alpha = 0.02 \pm 0.04$; i.e., the average diameter was constant within experimental uncertainty at 5.3 ± 0.4 μm. The $\alpha = 0$ power law is necessary for continuous dropwise condensation with effective heat transport. In conventional dropwise condensation, the steady-state condition with constant average diameter is typically accomplished with gravity on a *tilted* hydrophobic surface, leading to an average drop diameter well above 100 μm [2,4]. On the horizontal superhydrophobic surface reported here, autonomous drop removal was observed to result from coalescence involving at least one "large" drop with diameter $\gtrsim 10$ μm [19]. This critical drop diameter for mobile coalescence probably dictates $\langle 2r \rangle$ in the same manner that the capillary length does in conventional dropwise condensation [4].

The rapid drop motion during Stage 3 condensation on the superhydrophobic substrate was studied by high-speed imaging, and a surprising out-of-plane jumping motion upon coalescence was captured. Repeated observations confirmed that the condensate departed the surface only after coalescing with other drops. Two types of mobile coalescence were observed: *initial coalescence* where a static group of neighboring drops merged together and departed the surface (Fig. 3), and *dynamic coalescence* where a drop already in motion from a previous coalescence came in contact with a stationary drop(s) (Fig. 4). Although the merged drop exhibited a lateral velocity as high as 1 m/s (e.g., when several drops initially coalesced in Fig. 3), its velocity was typically dominated by the vertical component as shown in Fig. 4. Although it has been observed elsewhere that condensate drops can mobilize individually on a substrate near its melting point [20] or collectively upon coalescence on a superhydrophobic surface [8–10], this is the first report of an out-of-plane jumping motion spontaneously occurring on engineered surfaces.

The surface coverage on the superhydrophobic surface was not dramatically lower than that on its hydrophobic counterpart due to the appearance of new families of droplets [11]; however, this recreation of the early droplet growth cycle leads to very efficient heat removal [3]. Because the heat transfer rate increases with decreasing average drop diameter even with the same surface coverage [2,4,21], superhydrophobic surfaces can be used to promote effective dropwise condensation. Although the jumping phenomenon occurred at all orientations, the sub-

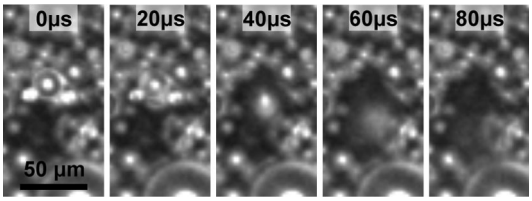

FIG. 3. Top-down imaging of autonomous drop removal via initial coalescence. A group of initially static condensate drops coalesced together and subsequently moved out of focus, indicating an upward trajectory over the surface. The largest drop in the group has a diameter of 15 μm, and the lateral speed was approximately 1 m/s. See video S3 in [33].

strate was horizontally oriented here to show that no external force is needed for condensate removal: the merged drop jumped off the surface, fell back in the mobile Cassie state [22], and bounced across the surface until it triggered another coalescence. After a few coalescences, the merged drops moved out of the field of view (0.4×0.4 mm^2) and eventually rolled off the chip (20×20 mm^2).

The self-propelled drop motion appears to be powered by the surface energy released upon drop coalescence. On a superhydrophobic surface, the condensate drops can be assumed spherical to first order approximation with negligible interactions with the substrate. If all of the released surface energy is converted to translational kinetic energy, when two spherical drops of radii r_1 and r_2 coalesce into one, the velocity of the merged spherical drop is

$$v_i = \sqrt{\frac{6\sigma}{\rho}\frac{r_1^2 + r_2^2 - (r_1^3 + r_2^3)^{2/3}}{r_1^3 + r_2^3}}, \tag{2}$$

where σ is the surface tension and ρ is the density of the liquid. For drops of equal radius, $r_1 = r_2 = r$, this inertial-capillary velocity reduces to

$$v_i \propto \sqrt{\sigma/\rho r}. \tag{3}$$

When inertia dominates, the merging time scales as

$$t_i \propto \sqrt{\rho r^3/\sigma}. \tag{4}$$

Similar inertial-capillary velocity and time scales have proven useful in inertia-dominated problems involving the bridge formation during drop coalescence [23,24] and the bouncing motion of superhydrophobic drops [25,26]. The Reynolds number based on v_i is

$$\mathrm{Re}_i \propto \sqrt{\sigma\rho r/\mu^2}, \tag{5}$$

where μ is the liquid viscosity. Therefore, viscosity dominates as the radius approaches a critical value,

$$r_{\mathrm{cr}} \propto \mu^2/\sigma\rho, \tag{6}$$

at which the inertial velocity v_i equals the viscous-capillary velocity of $v_v \propto \sigma/\mu$.

The vertical velocity of the merged drop resulting from coalescence of two individual drops was measured experimentally (Fig. 5). The measured velocity (v_{ex}) was nondimensionalized by the theoretical velocity [v_i in Eq. (2)],

$$v^\star = v_{\mathrm{ex}}/v_i. \tag{7}$$

For average drop diameter $2r_{\mathrm{avg}} \geq 85$ μm, the nondimensional velocity ($v^\star$) was approximately constant at 0.17. The measured Reynolds number was $\mathrm{Re} = 0.38$ at $2r_{\mathrm{avg}} = 17$ μm and 11 at 85 μm. The experimental results at relatively high Reynolds numbers ($\mathrm{Re} \gtrsim 10$) support the inertial-capillary velocity scaling [Eq. (2)]. The measured coalescence time was also on the same order as the inertial time scale. At lower Reynolds numbers, viscous effects became increasingly important, which explains the reduction in $v^\star$ (not necessarily in v_{ex}).

The experimentally observed critical diameter for jumping was of order 10 μm, much higher than the theoretical prediction which is of order 10 nm for water [Eq. (6)]. This discrepancy may be explained by the relatively weak dependence of the Reynolds number on drop size [Eq. (5)], together with the negligence of all dissipative processes including those related to the contact line movement [27,28] and the viscosity-dominated initial bridging process [23,29–31]. Interestingly, the critical size of the Buller's drop for triggering spore ejection is also 10 μm [6,7] despite the differences in the ejection and jumping processes.

The unusual out-of-plane motion resulting from in-plane coalescence was reproduced on a Leidenfrost surface [32]; see video S5 in [33]. On a hot surface liquid drops float on a vapor layer, resembling superhydrophobicity [26,34]. When two Leidenfrost drops coalesced, a liquid bridge formed above the substrate along the center line of the drops. The bridge diameter quickly grew to be larger than that of the original drops, and the impact of the liquid bridge on the substrate (or rather the compression of the vapor layer) exerted an upward force lifting the merged drop up. The millimetric Leidenfrost drops followed the same scaling trends [Eqs. (3) and (4)] as the much smaller superhydrophobic condensate drops. We believe the same "liquid bridge impacting substrate" mechanism is underlying the jumping motion on superhydrophobic surfaces, which is somewhat evident in video S4 [33]. This mechanism explains why the jumping motion has not been ob-

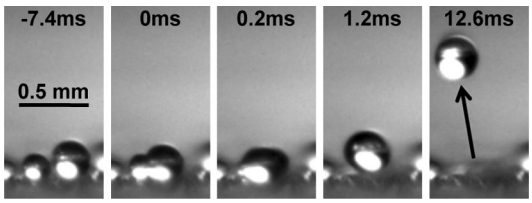

FIG. 4. Side-view imaging of autonomous drop removal via dynamic coalescence. The drop on the right with a diameter of 270 μm, mobile from a previous coalescence, moved into the static drop on the left with a diameter of 200 μm. Despite the in-plane coalescence at 0 ms, the merged drop propelled itself upward into the air with a vertical velocity of 0.14 m/s. The horizontal momentum was conserved. See video S4 in [33].

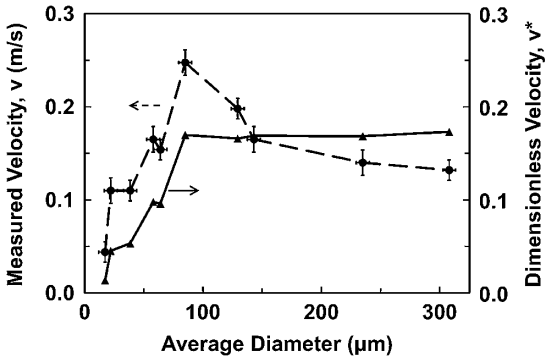

FIG. 5. Velocity of the merged drop vs the average diameter of two coalescing drops. The error bars of the measured velocity (●) were based on the video resolution. The nondimensional velocity (▲) indicates that the jumping velocity scales as v_i [Eq. (2)] above a critical diameter. For Fig. 5 only, a humidifier was sometimes used to accelerate the condensation process with negligible effect on the trend of the measured velocity.

served from drop coalescence on conventional substrates [27,35,36]. Our findings show that although surface roughness is critical for achieving superhydrophobicity, it is not essential for the jumping motion. However, the spontaneous motion offers a mechanism to switch from the sticky Wenzel state [37] to the nonsticking Cassie state [22], a transition crucial for achieving antidew superhydrophobicity on rough surfaces [38]. The surface energy released upon coalescence of two drops can be as high as 20% of the original energy, about 10 times larger than the typical energy barrier for Wenzel to Cassie transition [39].

In conclusion, we reported a self-propelled jumping motion of condensate drops on a superhydrophobic surface, and our scaling model suggested that such motion results from the surface energy released upon drop coalescence. The jumping leads to autonomous removal of dropwise condensate without the action of any external forces, which has the potential to enhance condensation heat transfer.

This work was funded by the National Science Foundation (CBET-08-40370) and the Pratt-Gardner Foundation. We thank X. Zhang for technical help.

*chuanhua.chen@duke.edu

[1] E. Schmidt, W. Schurig, and W. Sellschopp, Tech. Mech. Thermodyn. (Forsch. Ing. Wes.) **1**, 53 (1930).
[2] J. Rose, Proc. Inst. Mech. Eng., A J. Power Energy **216**, 115 (2002).
[3] J. Lienhard IV and J. Lienhard V, *A Heat Transfer Textbook* (Phlogiston, Cambridge, 2003), 3rd ed.
[4] J. Rose and L. Glicksman, Int. J. Heat Mass Transf. **16**, 411 (1973).
[5] A. Buller, *Researches on Fungi* (Longmans, Green, and Co., London, 1909), Vol. 1.
[6] J. Turner and J. Webster, Chem. Eng. Sci. **46**, 1145 (1991).
[7] A. Pringle *et al.*, Mycologia **97**, 866 (2005).
[8] C. Chen *et al.*, Appl. Phys. Lett. **90**, 173108 (2007).
[9] C. Dorrer and J. Ruhe, Adv. Mater. **20**, 159 (2008).
[10] B. Mockenhaupt *et al.*, Langmuir **24**, 13 591 (2008).
[11] D. Beysens, Atmos. Res. **39**, 215 (1995).
[12] For Figs. 1 and 2, the cold plate was initially at room temperature and was cooled to 5 °C by a chiller with precooled working fluid. The cold plate was approximately a lumped capacitance with a thermal RC time constant [3] of 8 s.
[13] C. Knobler and D. Beysens, Europhys. Lett. **6**, 707 (1988).
[14] R. Narhe and D. Beysens, Phys. Rev. Lett. **93**, 076103 (2004).
[15] R. Narhe and D. Beysens, Europhys. Lett. **75**, 98 (2006).
[16] D. Beysens and C. Knobler, Phys. Rev. Lett. **57**, 1433 (1986).
[17] D. Fritter, C. Knobler, and D. Beysens, Phys. Rev. A **43**, 2858 (1991).
[18] J. Viovy, D. Beysens, and C. Knobler, Phys. Rev. A **37**, 4965 (1988).
[19] It is a coincidence that the critical length scale is close to the micropillar dimensions. The condensation dynamics on a substrate with only nanoscale roughness were very similar to the two-tier roughness case reported here.
[20] A. Steyer, P. Guenoun, and D. Beysens, Phys. Rev. Lett. **68**, 64 (1992).
[21] A surface coverage approaching unity is implied in [4].
[22] A. Cassie and S. Baxter, Trans. Faraday Soc. **40**, 546 (1944).
[23] J. Eggers, J. Lister, and H. Stone, J. Fluid Mech. **401**, 293 (1999).
[24] M. Wu, T. Cubaud, and C. Ho, Phys. Fluids **16**, L51 (2004).
[25] D. Richard, C. Clanet, and D. Quere, Nature (London) **417**, 811 (2002).
[26] A. Biance *et al.*, J. Fluid Mech. **554**, 47 (2006).
[27] C. Andrieu *et al.*, J. Fluid Mech. **453**, 427 (2002).
[28] R. Narhe, D. Beysens, and Y. Pomeau, Europhys. Lett. **81**, 46 002 (2008).
[29] D. Aarts *et al.*, Phys. Rev. Lett. **95**, 164503 (2005).
[30] S. Case and S. Nagel, Phys. Rev. Lett. **100**, 084503 (2008).
[31] K. Fezzaa and Y. Wang, Phys. Rev. Lett. **100**, 104501 (2008).
[32] J. Boreyko and C. Chen (unpublished).
[33] See EPAPS Document No. E-PRLTAO-103-005945 for supplemental information. Videos S1 and S2 show dropwise condensation on the hydrophobic and superhydrophobic surfaces, respectively; video S3 shows the top-down imaging of initial coalescence; video S4 shows the side-view imaging of dynamic coalescence; video S5 shows the coalescence and jumping of Leidenfrost drops. For more information on EPAPS, see http://www.aip.org/pubservs/epaps.html.
[34] J. Leidenfrost, *De Aquae Communis Nonnullis Qualitatibus Tractatus* (Johann Straube, Duisburg, 1756).
[35] A. Menchaca-Rocha *et al.*, Phys. Rev. E **63**, 046309 (2001).
[36] W. Ristenpart *et al.*, Phys. Rev. Lett. **97**, 064501 (2006).
[37] R. Wenzel, Ind. Eng. Chem. **28**, 988 (1936).
[38] J. Boreyko and C. Chen, Phys. Rev. Lett. **103**, 174502 (2009).
[39] C. Ishino, K. Okumura, and D. Quere, Europhys. Lett. **68**, 419 (2004).